Analysis of Soil Parameters of Former Small-Scale Mining Land in Cempaka, Banjarbaru

Ishaq Ishaq[1*], *Dessy Lestari* Saptarini[1], and *M. Tommy* Maulidyanto[1]

[1]Department of Mining Engineering, Politeknik Negeri Banjarmasin, Banjarmasin, Indonesia

Abstract. The emergence of environmental problems on former small-scale mining sites, especially the potential formation of acid mine drainage, is closely related to the physical and chemical characteristics of the soil. Soil with a pH that is too low or too high can have a negative impact on the surrounding environment and ecosystem. Acidic soil, for example, often triggers the formation of acid mine drainage (AMD). This study aimed to examine the distribution of surface soil pH and resistivity at former mining areas, along with the correlation between these two soil properties. The research methods included field surveys, determining sample points based on a predetermined grid, and measuring physical parameters. The pH value was measured using a pH meter, while the resistivity was calculated based on the results of current (I) and potential difference (V) measurements using a simple multimeter, then the resistance (R) was derived and the resistivity (ρ) value was calculated. The data obtained were tabulated according to the sample point coordinates and analyzed descriptively and spatially using the Ordinary Kriging method. The results of the study showed that the soil pH values ranged from acidic to slightly neutral. The resistivity (ρ) values varied between sample points, with an inverse relationship to pH, i.e., the lower the pH value, the higher the soil resistivity tended to be. This condition reinforced the hypothesis that soil acidity levels affect resistivity (ρ) characteristics.

1 Introduction

In the Cempaka area of Banjarbaru City, small-scale community mining has long been one of the main sources of livelihood for local residents, passed down through generations until today. While this activity provides economic benefits, it also leaves behind several environmental challenges. One of the most significant issues is the alteration of soil characteristics, which can hinder the growth of surrounding vegetation or make it difficult for new plants to establish. This is largely due to an increase in soil acidity (pH), as soil pH directly influences the availability and uptake of nutrients by plants. Generally, nutrients are most easily absorbed within a pH range of 6–7, since most essential elements are more soluble in water under these conditions [1].

* Corresponding author: ishaq14@poliban.ac.id

Soils with extremely low or high pH levels can negatively impact the environment and surrounding ecosystems. Acidic soils, for instance, often trigger the formation of acid mine drainage (AMD), which occurs when sulfide minerals react with air and water, producing water with very low pH. AMD is typically formed through the oxidation of sulfide minerals such as pyrite and marcasite (FeS_2), which are exposed on rock surfaces and subsequently interact with rainwater or groundwater present at mining sites [2]. This condition not only reduces land productivity but can also contaminate water sources, damage vegetation, and disrupt the daily lives of nearby communities, particularly in terms of access to clean water.

The formation of AMD pollutes surface water bodies and alters the quality of soils in the surrounding area, where its acidity can be determined by measuring soil pH. In addition, soil resistivity (ρ), which is inversely related to soil pH [3], can serve as a comparative parameter when assessing the characteristics of post-mining soils. The main objective of this study is to analyze the characteristics and spatial distribution of soil pH and soil resistivity in abandoned community mining areas in Pumpung Village.

High soil acidity is also closely associated with high base saturation levels. Soils with low base saturation often have their exchange complexes dominated by acidic cations such as Al^{3+} and H^{+}. When these acidic cations accumulate in excessive amounts, they can become toxic to plants. Such conditions are typically found in strongly acidic soils [4].

In the former small-scale mining area of Cempaka, particularly in Pumpung Village, quantitative information regarding the spatial relationship between soil pH and resistivity based on geostatistical approaches remains unavailable. To date, no integrated mapping has been conducted using variogram analysis and kriging interpolation to characterize the spatial distribution and continuity of these parameters. This condition results in a partial characterization of soil affected by AMD, which remains unsupported by scientific data. This study therefore integrates soil pH and resistivity within a geostatistical framework to provide a more robust scientific basis for environmental management and post-mining land reclamation in small-scale mining areas.

2 Method

2.1 Location of the study area

This study was carried out in Pumpung Village, Cempaka District, Banjarbaru City, South Kalimantan, Indonesia, located close to residential areas. The research site is shown in the map provided in **Fig. 1**.

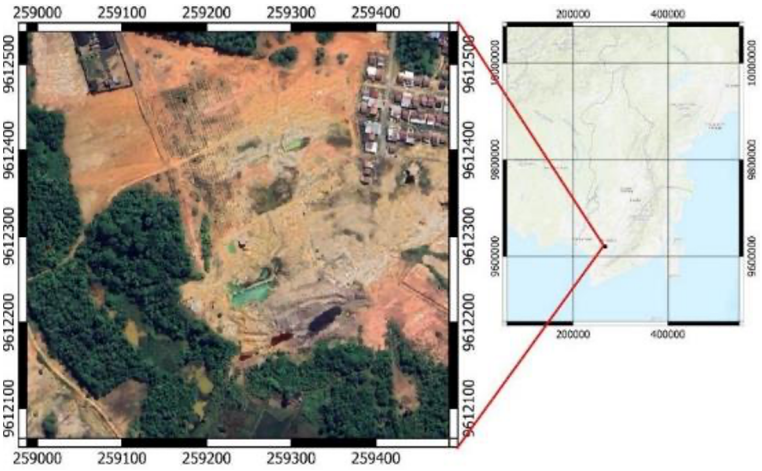

Fig. 1. Location map of the study area

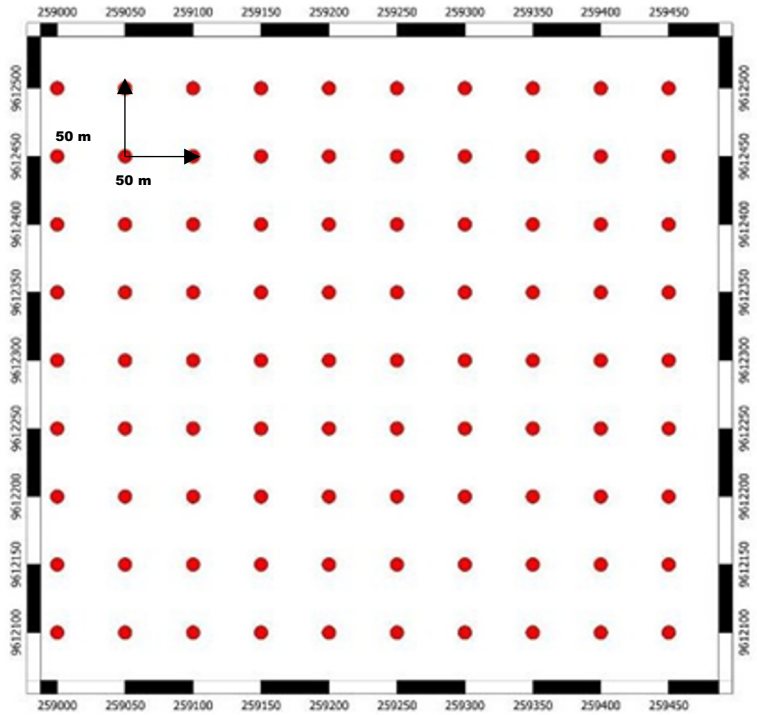

Fig. 2. Sampling design plan

2.2 Research data

This study is categorized as primary research, in which the data were directly collected and measured in the field. The parameters observed include soil acidity (pH) and surface soil resistivity (ρ) in former mining areas. **Fig. 2** presents the planned sampling point layout in the field, with a spacing of 50 meters and the number of pH is 121 and soil resistivity is 121 data at identical sampling locations.

2.3 Data acquisition

Soil resistivity was measured **Fig. 3** using a multimeter configured to record current (I) and potential difference (V), from which the resistance (R) could be calculated using the following equation:

$$R = \frac{V}{I} \quad (1)$$

Considering the geometric factor in the measurement, where the electrode spacing is denoted as a (with a = 5 cm in this study), the actual soil resistivity can be calculated using the following equation:

$$\rho = 2.\pi.a\left(\frac{\Delta V}{I}\right) \quad (2)$$

where ρ = resistivity (Ω·m), ΔV = potential difference (V), I = injected current (A), and a = spacing between the current and potential electrode pairs (m) [5].

Soil pH was measured directly in the field using a pH meter at the same time as soil resistivity (ρ) measurements at the same coordinates. For resistivity measurements, two multimeters (one for current and one for potential difference) were used, arranged as shown in **Fig. 2**, to obtain the soil resistivity (ρ) values directly at the sampling points.

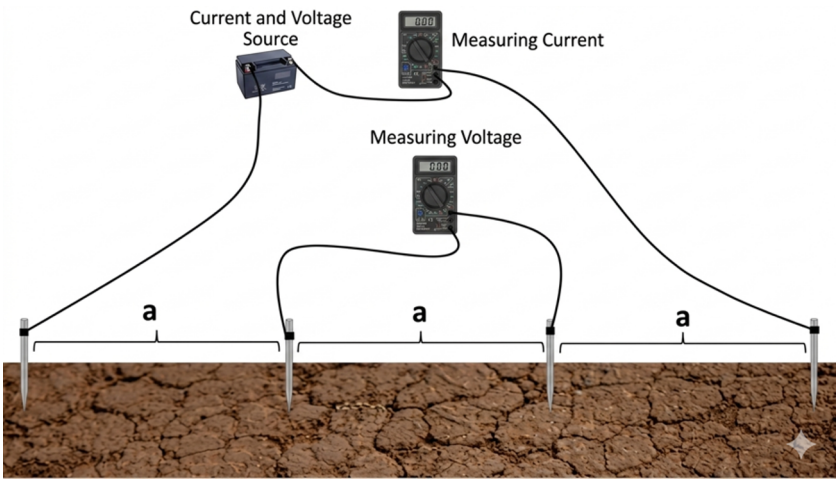

Fig. 3. Multimeter Configuration for Soil Resistivity Measurement

2.4 Data analysis

Data processing was carried out using SGeMS v2.1. The experimental variogram was first computed based on the measured dataset, followed by a variogram fitting procedure in which several theoretical models were compared. The spherical model was selected because it provides a more realistic representation of the spatial continuity structure of the data, consistent with the characteristics of geoscientific data (e.g., soil parameters) as reflected in the empirical variogram [6].

3 Results and discussion

3.1 Results

Descriptive data analysis was carried out to examine the characteristics of soil pH and resistivity values as shown in **Table 1** and **Table 2**.

Table 1. Descriptive statistics of soil pH

pH	
Variables	**Values**
Mean	5.9
Standard Error	0.0
Median	6.0
Mode	6.0
Standard Deviation	0.5
Sample Variance	0.3
Kurtosis	0.5
Skewness	-1.2
Range	2.0
Minimum	4.5
Maximum	6.5
Count	121

Table 2. Descriptive statistics of soil resistivity

Soil Resistivity (ρ)	
Variables	**Values**
Mean	7.1
Standard Error	0.4
Median	6.4
Mode	7.9
Standard Deviation	4.0
Sample Variance	16.1
Kurtosis	3.6
Skewness	1.4
Range	23.8
Minimum	2.1
Maximum	26.0
Count	121

Subsequently, histogram analysis was performed for both parameters in order to identify the data distribution. The resulting histograms for each parameter are presented in **Fig. 4 (a)** and **Fig. 4 (b)**.

Next step, variogram analysis was conducted to examine the spatial structure of soil pH and resistivity (ρ) at the study site, allowing us to determine the extent to which a parameter remains spatially correlated. The nugget represents the amount of local variability unexplained by distance, the sill indicates the maximum level of variability, and the range defines the distance over which a parameter still shows spatial dependence.

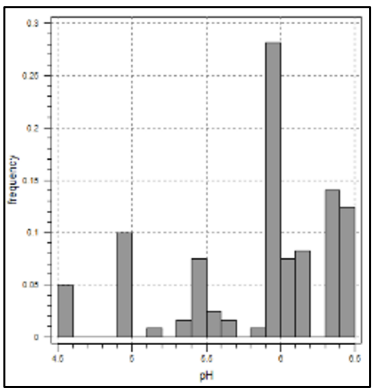

Fig. 4. (a) Histogram soil pH

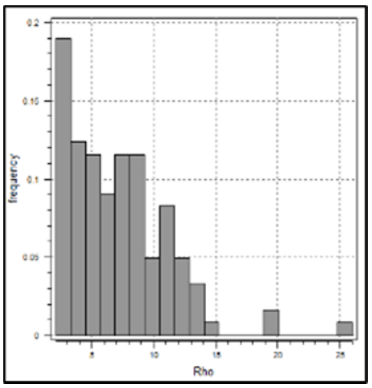

Fig. 4. (b) Histogram resistivity

The spatial structure is represented by the variogram γ(h). The variogram describes the average variance between observed data points separated by distance h, and is formulated as follows [7,8]:

$$\gamma(h) = \frac{1}{2N(h)} \sum_{i=1}^{n} \{Z(x_i) - Z(x_i + h)\}^2 \quad (3)$$

where:

$Z(xi)$: Measurement at location xi
$Z(xi + h)$: Measurement at location $xi + h$
$\gamma(h)$: Variogram for the distance h between $Z(xi)$ with $Z(xi + h)$
$N(h)$: Number of data pairs separated by distance h.

The pH variogram use spherical model with a nugget of approximately 0.12, a sill of 0.30, and a range of about 260 meters. The relatively high nugget suggests local heterogeneity or measurement uncertainty at short distances. The sill value of 0.30 reflects the maximum variability captured by the pH data, while the range of about 260 meters marks the limit of spatial autocorrelation. In other words, pH values remain spatially related up to a distance of 260 meters, beyond which they become random or uncorrelated.

The soil resistivity variogram use spherical model with a nugget of about 7, a sill of 20, and a range of approximately 500 meters. The relatively high nugget indicates local heterogeneity or measurement uncertainty at short distances. The range of 500 meters suggests that soil resistivity remains spatially correlated up to this distance, after which its variation becomes random. This implies that resistivity has a longer spatial correlation compared to pH, meaning that resistivity values in the field tend to be more stable over larger spatial scales.

In this study, the variogram results show that soil pH has a shorter spatial correlation, meaning its values tend to fluctuate more rapidly across the field. On the other hand, soil resistivity displays a longer spatial correlation, indicating a more stable distribution over greater distances. Therefore, the use of variograms in spatial modeling is crucial for generating representative maps of soil pH and resistivity, which can then serve as a foundation for further analysis.

Linear regression was also applied to examine the correlation between the two physical parameters. The relationship between soil resistivity (ρ) and soil pH is presented in the **Fig. 5**.

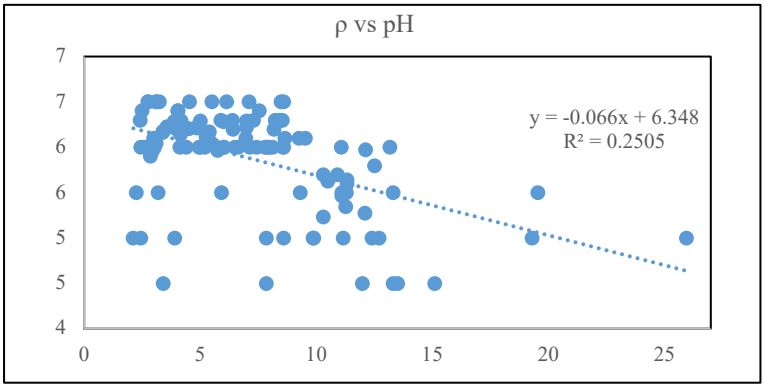

Fig. 5. Correlation between soil resistivity (ρ) and pH

Overall, the relationship between pH and soil resistivity (ρ) shows an inverse pattern, with a coefficient of determination (R^2) of 0.2505. This means that soil resistivity (ρ) and soil pH have a linear relationship of about 25.05%, expressed by the regression equation pH = –0.066ρ + 6.348. In other words, the correlation coefficient is –0.5014. The significance of the correlation coefficient was tested using the t-distribution with degrees of freedom (df = n – 2). With a total of n = 121 observations, the degrees of freedom were 119. The test statistic was calculated using the following equation [9]:

$$t = \frac{r\sqrt{n-2}}{\sqrt{1-r^2}} \quad (4)$$

With a value of r = –0.5014, the calculated t value is –6.32. At a significance level of α = 0.05, the t table value for df = 119 is ±1.98 and the calculated t (6.32) is greater than the t table (1.98), so the negative relationship between soil pH and resistivity (ρ) is declared statistically significant. This result indicates that the inverse relationship obtained does not occur by chance, but rather indicates a linear relationship between the two variables. These findings are consistent with previous studies, which reported that lower soil pH values tend to be associated with higher resistivity (ρ).

3.2 Discussion

3.2.1 Spatial Characteristics of Soil Resistivity and pH

Ordinary Kriging is an estimation method that does not consider the sample mean. In principle, assuming there are nnn samples at positions z(x_i), the estimation of the value at x_0 is expressed as follows:

$$Z_{OK}(x_0) = \sum_{i=1}^{N} \lambda_i \,.\, z(x_i) \quad (5)$$

To obtain an unbiased estimated value, the sum of the weighting factors is set to equal 1, expressed by the following equation [6]:

$$\sum_{i=1}^{N} \lambda_i = 1 \quad (6)$$

The results of Ordinary Kriging indicate variations in the spatial distribution of soil pH across the study area. Based on the distribution map **Fig. 6**, soil pH values range from 4.5 to 6.5, showing diverse spatial patterns. The central to northern parts are dominated by blue shades, representing low pH values (acidic soils), while the southern area shows relatively higher pH values approaching neutral, illustrated by yellow to red color gradients. This distribution pattern reflects the heterogeneity of soil chemical properties in the former small-scale mining area, which is likely influenced by differences in mining residues, sulfide mineral content, and the degree of oxidation that has occurred.

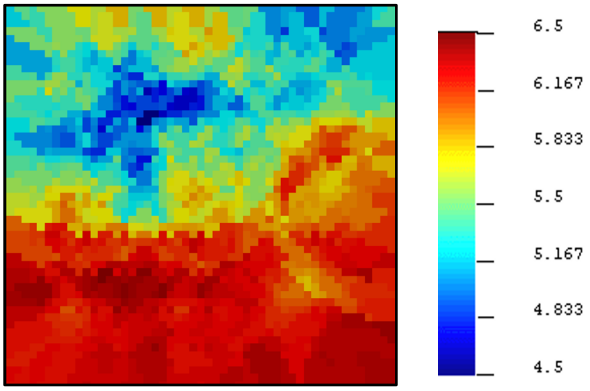

Fig. 6. Spatial analysis results soil pH

Meanwhile, the spatial distribution map of soil resistivity **Fig. 7** shows an opposite pattern compared to the pH distribution. Soil resistivity values range from 2.1 to 26 ohm·m, where dark blue areas represent low resistivity, while yellow to red areas indicate high resistivity. In general, areas with low pH tend to have higher resistivity, whereas areas with pH values closer to neutral show lower resistivity. This pattern highlights the inverse relationship between soil acidity and resistivity, where more acidic soil conditions correspond to higher resistivity values.

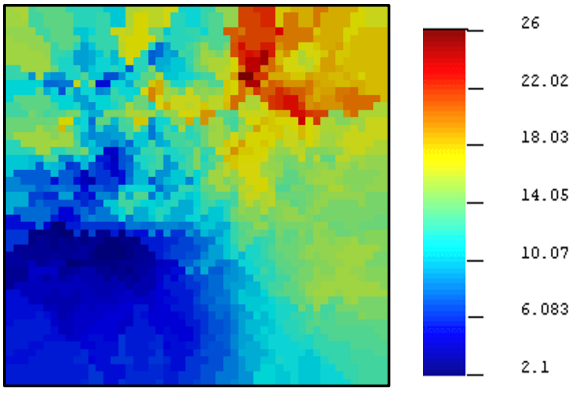

Fig. 7. Spatial analysis results soil resistivity

The spatial characteristics derived from the Ordinary Kriging interpolation indicate that the distribution of soil pH and resistivity values is not uniform, but instead forms

distinct zonation patterns. The relatively sharp gradients observed between different areas suggest that the soil conditions in the former mining site are strongly influenced by local factors, including both geological settings and previous mining activities. The application of geostatistical methods allows for the estimation of values at unsampled locations, thereby providing a more comprehensive understanding of the study area's land conditions.

3.2.2 Spatial distribution soil pH and resistivity

The soil pH distribution map **Fig. 8** shows acidity variations across the former small-scale mining area in Cempaka. Low pH values (4.5–5.0), indicated by blue to dark blue shades, are concentrated in the central and northern zones, reflecting highly acidic soils. Higher pH values (6.0–6.5), shown in red to yellow, in the southern. This pattern demonstrates spatial heterogeneity influenced by mining residues, sulfide mineral weathering, and ion leaching. The dominance of low pH in the central–northern area making it susceptible to the AMD.

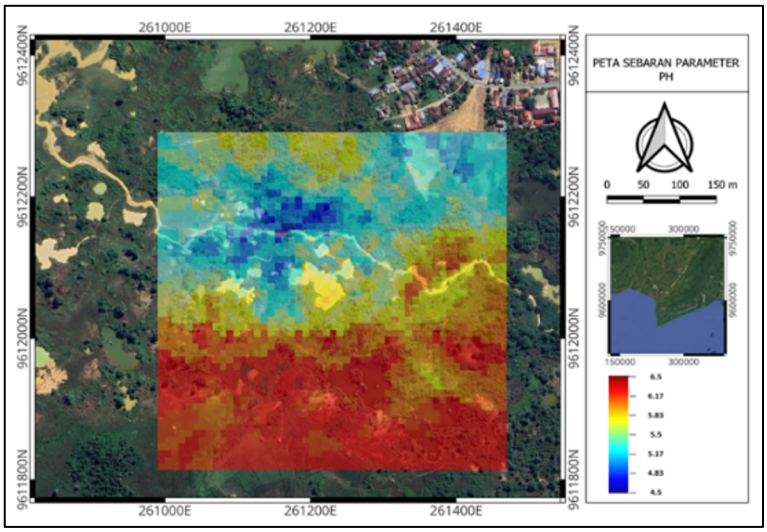

Fig. 8. Spatial distribution of soil pH the study area

The soil resistivity map **Fig. 9** ranges from 2.1 to 26 ohm·m. Low resistivity (<10 ohm·m), depicted in blue shades, is primarily distributed in the southern–western areas and likely reflects higher dissolved ion concentrations. In contrast, high resistivity values (>20 ohm·m), shown in red to orange, are concentrated in the northern–northeastern zones and coincide with low pH areas. This pattern indicates that acidic soils tend to exhibit higher resistivity, possibly the research area is located in a tropical region with high rainfall, causing the leaching and dissolution processes at the soil surface to occur more rapidly.

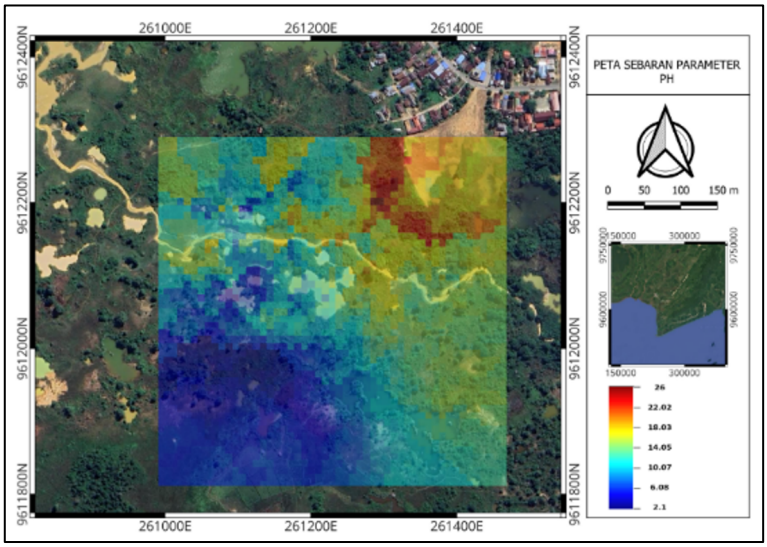

Fig. 9. Spatial distribution of soil resistivity in the study area

Thus, the spatial distribution maps of pH and resistivity generated through Ordinary Kriging provide a clear picture of the heterogeneity of former mining lands and can be utilized for zoning areas with potential risks of acid mine drainage (AMD) formation. Areas characterized by low pH and high resistivity can be prioritized for remediation programs, such as liming, to prevent the development of AMD that could contaminate the surrounding environment.

In addition, the inverse spatial relationship between pH and soil resistivity with R^2 = 0.2505 indicates that the linear model only explains 25.05% of the data variation, while the majority is influenced by other factors. This means that the relationship between the two is systematic but not deterministic, which is only fully determined by one variable. Water content, porosity, texture, mineral content, and ion content (salinity) of the soil also influence the control of resistivity values [10]. Thus, the tendency for increasing resistivity at low pH needs to be understood in the context of a complex soil system with various controlling variables.

4 Conclusion

The spatial distribution pattern shows that low pH (acidic soils) is predominantly found in the central to northern parts of the study area, while relatively higher pH values occur in the southern region. Conversely, high resistivity values are more dominant in areas with low pH, whereas lower resistivity values are distributed in areas with more neutral pH conditions. The correlation analysis between pH and resistivity reveals an inverse relationship, where decreasing soil pH tends to correspond with increasing resistivity. This indicates that soil acidity influences resistivity characteristics, reflecting the physical conditions of the soil.

References

1. Karamina, H.; Fikrinda, W.; Murti, A.T. Kompleksitas Pengaruh Temperatur Dan Kelembaban Tanah Terhadap Nilai PH Tanah Di Perkebunan Jambu Biji Varietas Kristal (Psidium Guajava l.) Bumiaji, Kota Batu. *Kultivasi* **2018**, *16*, doi:10.24198/kltv.v16i3.13225.
2. Rukmana, B.T.S.; Haq, S.R.; Lusantono, O.W. Pemanfaatan Mikroalga Dan Typha Untuk Penanganan Air Asam Tambang Pada Pertambangan Batubara. *J. Teknol. Pertamb.* **2026**, *11*, 36–45, doi:10.31315/jtp.v11i2.16030.
3. Seputra, I.; Wijaya, I.; Janardana, I. Pengaruh Potensial Hidrogen (PH) Tanah Terhadap Tahanan Jenis Tanah Untuk Mendapatkan Bentuk Sistem Pembumian. *J. SPEKTRUM* **2019**, *6*, 29, doi:10.24843/SPEKTRUM.2019.v06.i04.p5.
4. Mahendra, D.; Sulakhudin, S.; Chandra, T.O. Identifikasi Sifat Kimia Tanah Pada Areal Penambangan Kaolin Di Desa Pawangi Kecamatan Capkala Kabupaten Bengkayang. *J. Sains Pertan. Equator* **2024**, *13*, 1061–1071, doi:10.26418/jspe.v13i4.69959.
5. Santoso, B. Identifikasi Korosivitas Tanah Menggunakan Metode Resistivitas Wenner-4 Pin. *J. Ilmu dan Inov. Fis.* **2023**, *7*, 137–144, doi:10.24198/jiif.v7i2.43976.
6. Wani, O.A.; Sharma, V.; Kumar, S.S.; Malik, A.R.; Pandey, A.; Devi, K.; Kumar, V.; Gairola, A.; Yadav, D.; Valente, D.; et al. Geostatistical Modelling of Soil Properties towards Long-Term Ecological Sustainability of Agroecosystems. *Ecol. Indic.* **2024**, *166*, 112540, doi:10.1016/j.ecolind.2024.112540.
7. Ishaq, I. Efektivitas Ordinary Cokriging Dan Kriging Untuk Karakterisasi Potensi Manifestasi Panas Bumi. *J. INTEKNA Inf. Tek. dan Niaga* **2018**, *18*, 79–85.
8. Myers, D.E. Basic Linear Geostatistics. *Technometrics* **2000**, *42*, 437–437, doi:10.1080/00401706.2000.10485732.
9. Fischer, P.; Berg, E.; Hopmann, C.; Dahlmann, R. Investigating the Impact of Seasonal Input Stream Fluctuations on Post-Consumer High-Density Polyethylene Composition and Processing. *Polymers (Basel).* **2025**, *17*, 1828, doi:10.3390/polym17131828.
10. Sangprasat, K.; Puttiwongrak, A.; Inazumi, S. Review of Correlations Between Soil Electrical Resistivity and Geotechnical Properties. *Geosciences* **2025**, *15*, 166, doi:10.3390/geosciences15050166.